Nanoscale

Plasmon-mediated Discrete Diffraction Behaviour of an Array of Responsive Waveguides

Journal:	*Nanoscale*
Manuscript ID	NR-ART-08-2019-006917.R1
Article Type:	Paper
Date Submitted by the Author:	05-Sep-2019
Complete List of Authors:	Pezzi, Luigia; CNR, CNR Nanotec De Sio, Luciano; Sapienza University of Rome, Department of Medico-surgical Sciences and Biotecnologies Veltri, Alessandro; Universidad San Francisco de Quito, Colegio de Ciencias e Ingeniería Cunningham, Alastair; Université de Genève, Département de Chimie Physique De Luca, Antonio; University of Calabria, Physics Bürgi, Thomas; Université de Genève, Department of Physical Chemistry Umeton, Cesare; University of calabria, Physics Caputo, Roberto; University of Calabria, Physics

Journal Name

ARTICLE TYPE

Cite this: DOI: 00.0000/xxxxxxxxxx

Plasmon-mediated Discrete Diffraction Behaviour of an Array of Responsive Waveguides

Luigia Pezzi,*[a‡] Luciano De Sio,[b,a,‡] Alessandro Veltri, [c] Alastair Cunningham, [d] Antonio De Luca, [e,a] Thomas Büergi, [d] Cesare Umeton, [e,a] and Roberto Caputo, [e,a]

Received Date
Accepted Date

DOI: 00.0000/xxxxxxxxxx

We investigate the discrete diffraction phenomenon in a Polymer-Liquid Crystal-Polymer Slices (POLICRYPS) overlaying a random distribution of gold nanoparticles (AuNPs, plasmonic elements). We study the propagation of a CW green laser beam through the waveguide structure as a function of beam polarization, laser intensity and sample temperature. It turns out that the plasmonic field created at the interface between AuNPs and POLICRYPS waveguides enables and stabilizes the optical field propagation within the responsive nematic liquid crystal channels. The active role of the liquid crystal is pointed out by a polarization, temperature and beam divergence experimental analysis and evidenced by a peculiar trumpet-shaped discrete diffraction pattern. Theoretical simulations confirm that the observed optical behavior is governed by the interaction of the nematic liquid crystal with optical and plasmonic fields.

1 Introduction

Diffraction of light usually leads to the spatial broadening of its initial intensity profile and can be controlled by modifying materials properties and/or configuration of the medium where the beam propagates. In particular, to control the spatial divergence of a given beam, it is necessary to act on the refractive index of the material. In free space, diffraction in the paraxial limit is always negative. This means that unusual features like diffraction cancellation, or change of its sign to a positive value, are only possible when considering the propagation of light in a linearly coupled array of one dimensional waveguides [1]. In such a discrete medium, diffraction assumes a discrete behaviour, following the same periodicity of the waveguide system and can show a change of sign or can even become zero valued.

Non-linear optical phenomena in waveguide arrays have been experimentally investigated [1–4] and theoretically interpreted [1,3–10] by exploiting models that refer to the "Fermi-Pasta-Ulam" approach to one-dimensional dynamical systems [11]; in this framework, the non-linearity is introduced as a pertubation to a primarily linear problem. Numerical models have been implemented by exploiting the Coupled-Mode Theory (CMT) [5,6], taking into account only nearest-neighbor interactions. By considering the n^{th} waveguide coupled only to the $(n+1)^{th}$ and $(n-1)^{th}$ adjacent channels, it has been shown that the optical field propagating in the n^{th} waveguide obeys a nonlinear difference-differential equation. The phenomenon is described via a 'coupling constant', which is proportional to an overlap integral of two adjacent modes [2,6]; in the continuum (or long-wavelength) approximation, this discrete process is described by the non-linear Schrödinger equation [6,12,13]. This approach has played an important role in understanding the observed effects, providing fundamental relations between those parameters (like array period and beam incidence angle) that control the discrete diffraction phenomenon [1,7,12]. In particular, it is possible to predict whether the propagating light beam experiences normal discrete diffraction (the beam spreads while propagating), anomalous discrete diffraction (a diffraction whose sign is opposite to that one usually exhibited in nature and the beam spreads while propagating, but some anomaly is observed) or if diffraction disappears (solitons or discrete solitons formation) [1–3,14–18]. In this paper, we present and discuss the first experimental characterization and theoretical modeling of the electromagnetic wave propagation in a complex waveguide configuration made of a 1D periodic POLICRYPS structure [19–22] (an acronym for Polymer-Liquid Crystal-Polymer Slices) overlaying a monolayer of randomly distributed gold nanoparticles (AuNPs), deposited on a glass substrate. The POLICRYPS contains a nematic liquid crystal (NLC) whose director alignment can be perturbed both by the presence of AuNPs and by the electric field of a light beam propagating in the structure [23]. The sample assumes a distinctive behaviour, since the optical response of

[a] CNR-Licryl Lab., NANOTEC Institute, 87036 Rende, Italy. E-mail: luigia.pezzi@cnr.it
[b] Department of Medico-surgical Sciences and Biotechnologies, Sapienza University of Rome,04100 Latina, Italy. E-mail: luciano.desio@uniroma1.it
[c] Colegio de Ciencias e Ingenieria, Universidad San Francisco de Quito, Quito, Ecuador
[d] Department of Physical Chemistry, University of Geneva, CH-1211 Geneva 4- Switzerland
[e] Department of Physics, University of Calabria, 87036 Rende, Italy
‡ These authors contributed equally to this work

the structure is modified during the light wave propagation: The presence of a NLC inside the POLICRYPS structure and AuNPs located underneath it makes the entire system extremely responsive to optical[24,25] and plasmonic[26–28] fields as well as to temperature variations induced in the sample.

Since the optical behavior of coupled waveguides depends on their geometrical parameters (periodicity, waveguide width and height[5,12,19,29,30]) and on the refractive index of the medium[30] between them, it is of particular interest to use a liquid crystal as such a medium. Indeed, NLC is an active soft-material whose refractive index value can be electro-optically controlled at will, by use of moderate amplitude electric fields (few $V/\mu m$)[23,24,31,32]; in particular, NLC is responsive also to the electric field associated to an electromagnetic wave propagating in the waveguide. This can give rise to the self-confinement of light in solitary waves (spatial solitons) that are coupled to the waveguide itself[33]. Achieving discrete diffraction in an array of waveguides containing NLC is particularly intriguing for the possibility to actively control the phenomenon and hence the optical behavior of an eventual device[33]. Here, we propose a novel system in which the presence of an interface, between the plasmonic elements layer and the POLICRYPS array containing the NLC waveguides, drastically influences the discrete diffraction behavior[34] of the system, resulting in unusual optical phenomena. In fact, due to the interplay of optical and plasmonic induced reorientation of the NLC waveguides, the involved system appears different from those ones reported in literature[29,30,35,36]. In order to model this novel configuration, we have implemented a numerical model which reproduces the beam propagation in a satisfactory quantitative way.

2 Experimental analysis

The system under investigation is a microcomposite structure (POLICRYPS[19,20]) composed of slices of almost pure polymer alternated to films of well aligned NLC. The periodic structure sits on a carpet of randomly-distributed and mono-dispersed Au spherical nanoparticles (20nm in diameter) (see Fig. 1(a)) creating an active interface able to support plasmon-mediated effects. The sample is fabricated by assembling a glass cell made of a substrate containing the monolayer of Au nanoparticles and another glass slide put at controlled distance from the first one (10μm) by means of glass microspheres. The conventional mixture used for POLICRYPS fabrication[37–39] (26wt% of NLC (BL001, by Merck) + 74$wt\%$ of UV sensitive pre-polymer (NOA61, by Norland)) is then introduced in the cell by capillary flow. The spatially periodic POLICRYPS structure is obtained by irradiating the prepared cell (infiltrated with the pre-polymer mixture) with a curing interference pattern of UV/visible light under suitable experimental and geometrical conditions. The angle between the two interfering curing beams is set to obtain a POLICRYPS with a waveguide periodicity of about 5μm. The effect of the periodically modulated refractive index profile of the structure[19,20] can be switched on and off by applying an external electric field of the order of few $V\mu m^{-1}$.

Fig. 1(b) is a photograph of the fabricated sample, under ambient lighting conditions, highlighting the typical coloration (see

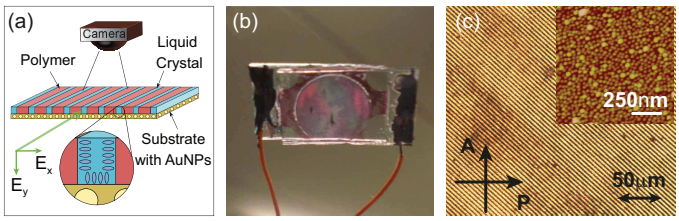

Fig. 1 Schetch, picture, POM view and morphology of investigated sample: (a) Schetch of the sample, the impinging light geometry and the acquiring set up, (b) Sample picture and (c) its Polarized Optical Microscope (POM) view with Atomic Force Microscope (AFM) morphology of the NP substrate underlying the POLICRYPS structure (inset).

circular spot in the middle) of the produced periodic structure. Its morphology is inspected by a Polarized Optical Microscope (POM). Fig. 1(c) shows the POM view of the sample where a quite regular and uniform structure made of polymeric walls alternated to NLC films can be observed. The inset of Fig. 1(c) shows the atomic force microscopy (AFM) image of the underlying AuNPs layer (AuNPs are monodispersed with an average diameter of about 20 nm). The realized system is investigated by sending a collimated laser beam ($\lambda = 532nm$) at the entrance of one or more of the POLICRYPS channels in a waveguide configuration. As sketched in Fig. 1(a), during propagation in the structure, light scattered by the guides is acquired by a Leica Z16 APO macroscope (10x magnification and proper zoom factor) placed on top of the POLICRYPS structure. In order to unveil the complex interweaving of physical processes taking place in our system during light propagation, the active role played by the induced NLC reorientation is highlighted by three different analyses: 1. Polarization dependence; 2. Temperature dependence; 3. Beam divergence analysis.

Polarization dependence.

The discrete diffraction behavior of the system has been stud-

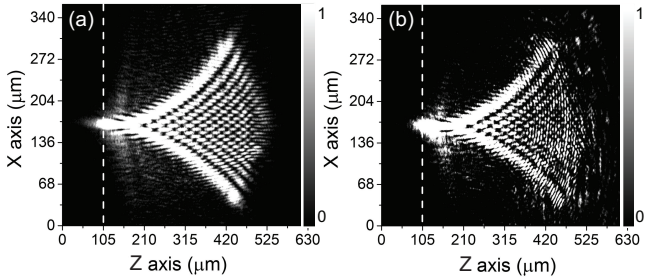

Fig. 2 Top view of light discrete behavior inside the POLICRYPS structure in waveguide configuration: polarization dependence: (a) p-polarized impinging light or transverse-magnetic polarization (TM) (b) s-polarized impinging light or transverse electric polarization (TE).

ied by irradiating few waveguides of the array with green light (wavelength $\lambda = 532nm$). In this analisys, discrete diffraction patterns are acquired while shining linearly polarized light in the waveguide system with two different polarization directions: p- or transverse-magnetic (TM) and s- or transverse-electric (TE) polarization, where transverse is referred to the propagation plane (x-z plane). These two polarization directions are indicated in Fig. 1(a) as Ex and Ey, respectively. The analysis of the discrete

diffraction behavior is performed by calculating the propagation length L in the central waveguide. The propagation length is defined as the distance between two consecutive maxima of light intensity in the central waveguide along the z-direction. It measures the length that light travels in a given waveguide before "jumping" to another one. Propagation of p-polarized light is shown in Fig. 2(a), where an anomalous discrete diffraction is observed, meaning that light is concentrated in two distinct outermost lobes[3]. In addition, a peculiar optical feature is observed: L changes during propagation, an effect evidently due to the active role of the NLC during light propagation. The black curve in Fig. 3 represents the propagation length value in the central waveguide of Fig. 2(a) as a function of the number of maxima. In Fig. 3, we see that this value decreases during the propagation, starting from the sample entrance (position 0) to the next jumps (from 1 to 8). Measures presented in Fig. 3 are obtained by converting images reported in Fig. 2 in digital data by using a suitable C++ code; this converts images in a matrix whose entries are values ranging from 0 to 1 where 0 correspond to dark and 1 to light and grays are in between. We then make a cut in the central waveguide (middle of the sample in x-direction) along the z propagation direction thus obtaining a $1D$ plot of the intensity modulation. Looking at Figs 2(a) and 3 we observe that L values

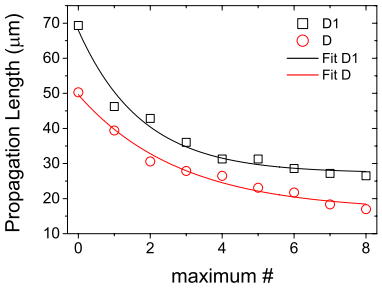

Fig. 3 Black squares (D1) and red circles (D) correspond to the experimental distances between maxima during the propagation of light in p-polarized configuration at room temperature Fig. 2(a) and 4(a) and at the nematic-isotropic transition temperature Fig. 4(b) respectively. Black (Fit D1) and red (Fit D) lines are the corresponding exponential fits.

decrease during light propagation. An explanation of this effect will be given later on in the theoretical paragraph. Different is the physical picture when s-polarized light is irradiating the guides. In this case, the electric field associated with the impinging wave tends to align the NLC molecules in the direction perpendicular to the sample substrate hence decreasing the refractive index mismatch between NLC and polymer. For this reason, even if the discrete diffraction starts in a way that is similar to the p-polarization case, the discrete pattern rapidly disappears, leaving an unclear light distribution that is probably due to interference effects more than discrete diffraction ones.

Temperature dependence.

Once verified that an interesting discrete diffraction behaviour is observed in presence of p-polarized impinging light, the same propagation experiment is studied while performing a temperature characterization of the sample. This is done by heating the sample up to the nematic-isotropic transition temperature of the NLC ($\sim 60^o$ C). A temperature increase lowers the NLC extraordi-

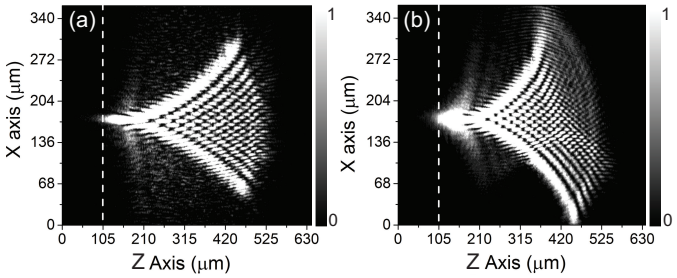

Fig. 4 Top view of light behavior inside the POLICRYPS structure in waveguide configuration in p-polarized configuration:(a) "trumpet" at room temperature in p-polarized light (b) bigger "trumpet" at $60^o C$ (transition nematic-isotropic temperature)

nary refractive index value bringing it close the ordinary one that is, in our case, very close to the polymer one. We acquire the light propagation images at room temperature (Fig. 4(a)) and at 60^o C (Fig. 4(b), nematic-isotropic transition temperature) and a visible change of the discrete diffraction pattern (trumpet-like shape) is observed. As resumed in the red curve of Fig 3, this is mainly due to a general decrease of the propagation length when increasing temperature. This result is coherent with the observation made in the polarization analysis, where a small refractive index mismatch between NLC and polymer results in shorter propagation lengths. It is also worth noting that, despite at 60^o C the NLC is expected to be in the isotropic state, the discrete diffraction pattern sensibly changes but does not disappear. We suppose that the p-polarized light propagating in the guides excites a strong plasmonic dipolar field in the AuNPs substrate[40]. This field prevents the NLC thermal fluctuations, thus favoring the director reorientation induced by the optical field[24,25,41]. The collective excitation of strongly coupled plasmonic particles during energy propagation in waveguides is well known and has been investigated in details in[40] where the efficiency of energy transport along the waveguide, due to surface plasmonic coupling, is studied for different dimensions and shapes of samples. Moreover, it has been demonstrated that the near-field coupling between particles distributed in arrays produces a guiding effect of electromagnetic waves at optical frequencies in presence of metal-dielectric interfaces[42]. These strong distance-dependent interactions lead to a splitting of the plasmon dipolar peak for regular one-dimensional arrays of metal nanoparticles[42]. Furthermore, in[43], Maier et al. experimentally show the coupling of the evanescent wave in a tapered optical fiber to a metal nanoparticle plasmon waveguide. The high efficiency of power transfer into these waveguides solves the coupling problem between conventional optics and plasmonic devices. By repeating the same characterization at higher beam intensities, we observe the same behavior but with longer propagation lengths (images not reported).

Beam divergence analysis.

A further interesting information is provided by a beam divergence analysis. Fig. 5(a) shows that light propagating in our samples exhibits anomalous discrete diffraction also in a non-paraxial configuration (when many waveguides are illuminated). In this case, in order to get a detailed insight of the light propagation behavior, the discrete diffraction pattern is acquired for different

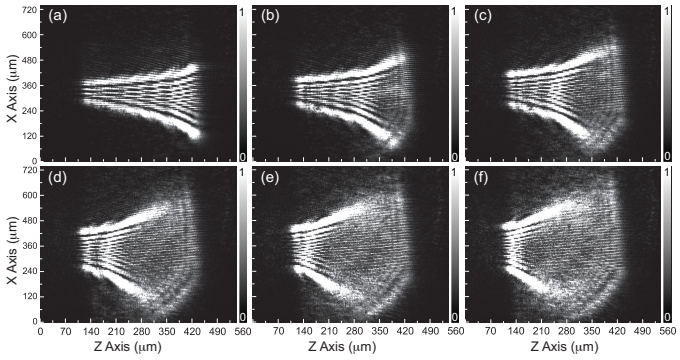

Fig. 5 Top view of light behavior inside the POLICRYPS structure in waveguide configuration at different temperature $T_0 < T_1 < T_2 < T_3 < T_4 < T_5$ with a divergent beam from (a) at $T_0 = 23^o C$ temperature (room temperature) to (f) at $T_5 = 60^o C$ (nematic-isotropic transition).

temperature values ranging from 23^o to 60^o C (Figs. 5a-f). In Fig. 5, it is possible to observe that, along the propagation direction, the region where the anomalous discrete diffraction takes place reduces with increasing temperature, turning to a normal, non-trumpet shaped, discrete diffraction (shown in[32] and theoretically predicted in the following paragraph (Figs. 7(a),(b)). It is interesting to note that, as already observed in Fig.4(b), notwithstanding the increase in the sample temperature, the role of the LC does not vanish: indeed, albeit small, a region of anomalous discrete diffraction is always present. This indicates that, although the temperature increase reduces the average value of the LC refractive index, light induces some reorientational plasmonic effects in the NLC director that preserves the anomalous discrete diffraction behaviour.

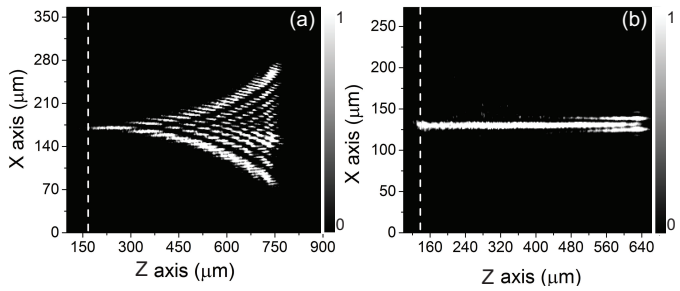

Fig. 6 Top view of light behavior inside the POLICRYPS structure in waveguide configuration at room and nematic-isotropic transition temperature ($23^o C$, $60^o C$) with a convergent beam. (a) at $T_0 = 23^o C$ temperature (room temperature). (b) at $T_5 = 60^o C$ (nematic-isotropic transition).

The last experimental analysis is performed in a paraxial configuration, in which exclusively one waveguide is excited by the laser beam (Fig. 6). At room temperature (Fig. 6(a)), the "trumpet" shaped pattern is very similar to that reported in Fig. 2(a). Quite different is, on the contrary, the pattern observed at the nematic-isotropic transition temperature, where anomalous discrete diffraction is almost completely suppressed and a soliton-like beam appears(Fig. 6(b))[44,45]. This confirms that a suitable temperature increase can cancel the periodicity of the refractive index, while light creates its own waveguide through a self-modulation of the refractive index, giving rise to a "nematicon-like" behavior[46,47]. In our opinion, this behavior is a further demonstration that the plasmonic field stabilizes the waveguiding effect of the NLC (by reducing thermal fluctuations) only in those areas where the impinging light excites a plasmonic response.

3 Theoretical model

In our theoretical analysis, the POLICRYPS structure is modeled as a system with a periodic dielectric permittivity profile (Fig 8). The light wavevector **k** is assumed parallel to the single waveguide of the array (see Fig. 1(a)) while the (p-polarized) electric field is oriented along the x axis in the plane of the structure; this enables modeling the system with a 2D approach. In this geometry, within the LC films of the POLICRYPS structure, light "sees" the extraordinary refractive index of the NLC, whose director alignment is induced by the polymeric boundaries[48], i.e. perpendicularly to the polymer slices. Thus, in a first theoretical approach we assume a periodic alternation of polymer refractive index and extraordinary index of the NLC. Light modes confined during the electromagnetic propagation are said "guided" waves (or guided modes) while structures supporting guided waves are called waveguides. The numerical implementation of the model takes into account the coupling between several parallel waveguides made of aligned liquid crystal films separated by polymer slices. Exchange of power between guided modes propagating in adjacent waveguides is referred to as directional coupling and is well explained by the coupled mode theory[5,49,50]. The Floquet-Bloch (FB) analysis predicts that the propagation-constant spectrum of the array's eigenmodes (the FB waves) is divided into bands, separated by gaps in which no propagating modes are allowed[50–52]. Light propagation in waveguide configuration is controlled by diffraction that, in free space, is governed by the equation $D_{np} = \frac{\partial^2 k_z}{\partial k_x^2} = \frac{-k^2}{(k^2 - k_x^2)^{3/2}}$ where D_{np} measures the broadening of the beam, (it is the difference in transverse shift between spatial frequency components) and **k** is the incident beam wavevector, with k_x, k_z being respectively its x- and z-components. In the paraxial limit ($k_x \approx 0$ and $k_z \approx k$), the previous equation gives $D_p = -1/k$[1]: meaning that D_p does not depend on k_x and is always negative. In case of the wave propagating in a linearly coupled, infinite array of one-dimensional waveguides, the diffraction relation can be derived using the framework of optical equivalence with the continuous model of tightly bound electrons in a one-dimensional atomic lattice[53]. The optically coupled mode set of equations for the electric field in the nth waveguide allows Yariv[5,12,49] to obtain the diffraction relation:

$$D_p = -2Cd^2 \cos k_x d \qquad (1)$$

where d is the periodicity of the structure and C is known as coupling parameter; the paraxiality is implicitly assumed in the derivation of expression (1) and is valid as long as $C \ll k$. It is evident from Eq. 1 that, when $\frac{\pi}{2} < |k_x d| \leq \pi$, the diffraction coefficient becomes positive, thus enabling light to experience "anomalous" discrete diffraction; this term meaning that most of light is gathered into two distinct outermost lobes and propagates by "jumping" from one waveguide to the external adjacent one. In

these conditions, light almost completely disappears in the region with low refractive index (see Fig. 7(a))[32]. On the other hand, by illuminating several waveguides, a non-paraxial condition holds, (Fig. 7(b)), which results in a negative (or normal) diffraction, characterized by a light intensity envelope that follows the laser beam gaussian profile, with non-zero intensity in the regions with low refractive index. Furthermore, in the two cases $k_x = \pm\frac{\pi}{2d}$ in Eq. 1, diffraction completely disappears, thus enabling soliton formation[3,32,45,54].

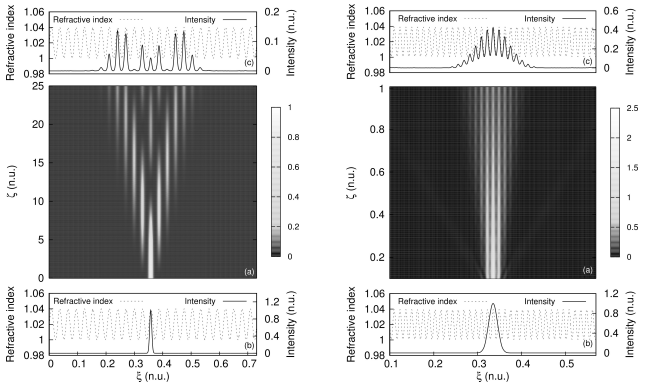

(a) anomalous (b) normal

Fig. 7 Anomalous and normal discrete diffraction in a coupled waveguides array.

By fixing the modulation Δn of the structure refractive index that gives rise to the system of adjacent waveguides, and using the coupled mode theory (CMT)[5], it is possible to show that, in a single waveguide, the power follows a sine-squared behavior (in the z-direction) and the distance between two maxima, in adjacent waveguides, depends on the wavelength λ of the impinging light, on the laser spot size w and on Δn. According to this theory, the light behavior is completely determined when we know the value of the coupling parameter C, whose expression, derived by Yariv[5,12,49,50,55], can be extended to subwavelength arrays[56]. Its expression is

$$C = \frac{2h^2 p\, e^{(-ps)}}{\beta(w_1 + \frac{2}{p})(h^2+p^2)} \tag{2}$$

where $h = \sqrt{n_1^2 k^2 - \beta^2}$, $p = \sqrt{\beta^2 - n_2^2 k^2}$, n_2 and n_1 are the refractive index of the waveguide and the adjacent medium respectively, $k = \omega/c$, β is the propagation constant, w_1 is the waveguide width, s is the distance between two adjacent waveguides. Using the coupled mode theory[49] it is possible to obtain the propagation lenght L simply as:

$$L = \frac{\pi}{2C} \tag{3}$$

Above mentioned models (CMT and FB) are very useful to carry out a discrete diffraction analysis in a structure whose refractive index exhibits a step profile, but they fail to account for key features of a POLICRYPS structure, where the refractive index has a smooth profile, determined by elastic forces and by the molecule anchoring conditions. In Fig. 8, we report the typical dielectric permittivity profile of a usual POLICRYPS structure. In this case,

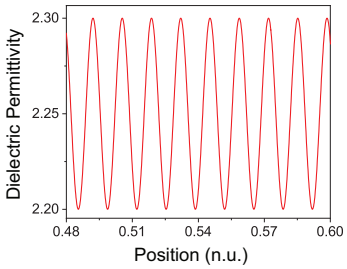

Fig. 8 Dielectric permittivity profile used to carry out the numerical simulation. The guides are made with a dielectric permittivity with gaussian profile in order to simulate the effective refractive index inside the liquid crystal channels.

in each waveguide, we have to use a gaussian transverse profile of the refractive index and a more suitable model is implemented to take account for our experimental conditions.

Description of the electromagnetic field propagation, derived through the Maxwell's spatial wave equation, is integrated with the additional terms: $\nabla\left(\mathbf{E}\cdot\frac{\boldsymbol{\nabla}\varepsilon}{\varepsilon}\right)$, because $\boldsymbol{\nabla}\varepsilon/\varepsilon$ is not negligible. Thus, the wave equation becomes

$$\boldsymbol{\nabla}^2\mathbf{E}(\mathbf{r}) + \omega^2\mu\varepsilon(\mathbf{r})\mathbf{E}(\mathbf{r}) = -\nabla\left(\mathbf{E}\cdot\frac{\boldsymbol{\nabla}\varepsilon}{\varepsilon}\right) \tag{4}$$

where $\mathbf{E}(\mathbf{r})$ is the electric field at position $\mathbf{r}$, ω is the angular frequency of light, μ is the magnetic permeability of the sample, that can be assumed as equal to that one of the vacuum, $\varepsilon(\mathbf{r})$ is the dielectric permittivity of the sample. If z is the wave propagation direction, by using a slab (planar) model, in which no variation exists in the y-direction, and assuming a "slow" envelope variation in z-direction, we can numerically solve equation (4) by taking into account the ε profile shown in Fig. 8 to write the refractive index modulation in the x direction. By considering solutions of the kind $\mathbf{E} = \mathscr{E}e^{i\beta z}$ we obtain, for the amplitude of the electric field:

$$\frac{\partial\mathscr{E}}{\partial\zeta} = \frac{i}{2\tilde{\beta}}\left[\frac{\partial^2\mathscr{E}}{\partial\xi^2} + \frac{1}{\varepsilon}\frac{\partial\varepsilon}{\partial\xi}\frac{\partial\mathscr{E}}{\partial\xi} + \frac{\partial}{\partial\xi}\left(\frac{1}{\varepsilon}\frac{\partial\varepsilon}{\partial\xi}\right)\mathscr{E} + (\tilde{k}^2 - \tilde{\beta}^2)\mathscr{E}\right] \tag{5}$$

where we introduced $\xi = x/W$ and $\zeta = z/W$ as the normalized spatial coordinates, W being the normalization length (i.e. the typical dimension of phenomenon), $\tilde{\beta} = W\beta$ is the normalized propagation constant and $\tilde{k} = 2\pi nW/\lambda$ is the normalized

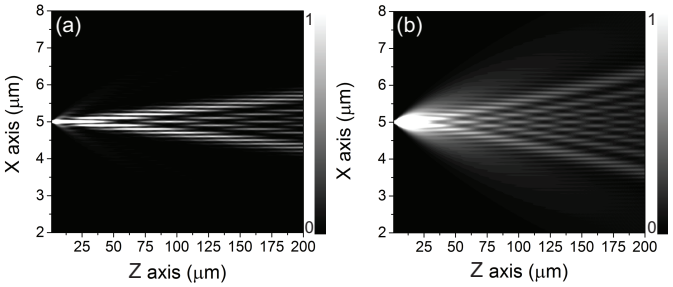

Fig. 9 Numerical result of light intensity propagation in a gaussian dielectric permittivity profile (like shown in Fig. 8) with average dielectric permittivity $\varepsilon_m = 2.25$ and variations (a) $\Delta\varepsilon_2 = 0.1$ and (b) $\Delta\varepsilon_1 = 0.01$

wavevector. In this equation we neglected the coupling between TE/TM modes because the electric field propagating in the waveguide is linearly polarized and parallel to the transverse coordinate (see[57], pag. 29)

We find the numerical solution of eq. 5 by imposing the gaussian profile of refractive index for each waveguide and using the finite differences method for the spatial derivatives. The system shows anomalous discrete diffraction with a propagation length value that is close to the experimental one. Moreover, we find that terms $\frac{1}{\varepsilon}\frac{\partial\varepsilon}{\partial\xi}\frac{\partial\mathscr{E}}{\partial\xi}$ and $\frac{\partial}{\partial\xi}\left(\frac{1}{\varepsilon}\frac{\partial\varepsilon}{\partial\xi}\right)\mathscr{E}$ are, in fact, not negligible, thus confirming the validity of our hypothesis.

To obtain a satisfactory agreement between measured and calculated propagation lengths, we assume an average dielectric permittivity of about $\varepsilon_m = 2.25$, with variations $\Delta\varepsilon_1 = 0.01$ or $\Delta\varepsilon_2 = 0.1$. Results are reported in Fig. 9, where an anomalous discrete diffraction behavior is evident with a longer propagation length corresponding to a larger birefringence value. We

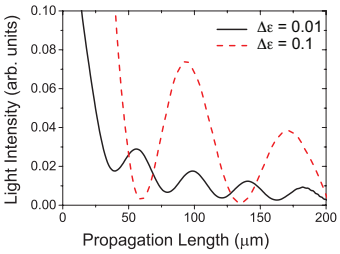

Fig. 10 Cuts in the central waveguide in the Fig. 9(a) (red dashed line) and Fig. 9(b) (black line)

highlight the difference in the propagation lengths by showing (Fig. 10) cuts of light intensity in the central waveguides of Figs 9(a) and 9(b). Differences in the propagation lengths are represented by different distances between maxima. It is well known that a temperature increase leads to a decrease of the extraordinary refractive index[58–63]; as such, Fig. 10 confirms the experimental result shown in Fig. 3, where lower propagation lengths correspond to higher temperatures hence, lower refractive index mismatch between LCs and polymer. As experimentally observed in Figs. 2, 4 and 6, the decrease of index mismatch, and thus of the propagation length, has a direct effect in the discrete diffraction pattern resulting in a "trumpet" shape. This peculiar pattern cannot be predicted by the actual code because it would require a recursive approach taking into account how local modifications of LCs orientation can influence the light intensity in that specific point. As indicated in Fig. 10, fixed values of the refractive index mismatch between LCs and polymer have been assumed in the simulations.

4 Discussion

In the study of the discrete diffraction taking place when light propagates in a POLICRYPS system of adjacent waveguides, the characterization of the polarization dependence upon wave propagation shows that, in the TM configuration of the impinging light, a discrete propagation with positive (anomalous) diffraction takes place while, in the TE configuration in the initial part of the waveguide, the discrete diffraction pattern shows the same features as in the TM case, but in propagation it becomes mixed up, probably due to some interference effect (Fig. 2). Our interpretation is that this is the result of the interplay between at least two phenomena. Indeed, the electric field direction of s-polarized light (TE mode) tends to align the NLC director in the direction perpendicular to the sample plane thus decreasing the index mismatch between NLC and polymer indices "seen" by the propagating light. Moreover, this field direction allows the propagating beams to interfere with each other thus modifying the discrete behavior during propagation. This hypothesis is reliable if it is assumed that, in the discrete diffraction, the polarization of light does not vary when the beam jumps from a waveguide to the adjacent one.

In a recent study the appearance of an anomalous discrete diffraction behavior, similar to the one observed here, has been interpreted as due to the presence of polaritons[35] (e.g. waves propagating along the surface of separation between metal and dielectric layers[26]). In our case, we can exclude such interpretation, since these waves can not propagate in the proposed configuration. Indeed, the gold layer underlying the POLICRYPS waveguides is not continuous but made of a carpet of randomly-distributed and mono-dispersed spherical nanoparticles. Thus, it can unlikely support polaritons propagation. Finally, temperature analysis results show that, at higher temperatures, observed propagation lengths are shorter (Fig. 3). In fact, at room temperature, light feels an effective LC refractive index quite close to the extraordinary refractive index of the BL001 NLC[62]. Then, an increase in temperature lowers the value of this index towards the isotropic value, with a consequent decrease of the birefringence and thus of the propagation lengths. This result is well confirmed by the implemented theoretical model (Fig. 10). However, an accurate observation of experimental results reveals that, at high temperature, when the NLC is expected to be in the isotropic state, the discrete diffraction pattern noticeably decreases but does not completely disappear. Behind this phenomenon, we have supposed a plasmonic contribution that prevents NLC thermal fluctuations thus stabilizing the NLC alignment even in conditions where this should be absent. From the beam divergence analysis (Fig. 5) it can be deduced that light intensity plays a fundamental role: where the beam is more intense (small divergence), discrete propagation is observed. In this case, light intensity affects the LC orientation thus modifying the birefringence of the structure. Theoretical analysis shows that the larger the birefringence of the structure, the longer the propagation length. This is in good agreement with the measured propagation lengths and their dependence on light intensity.

5 Conclusions

The propagation of light in an array of waveguides (Polymer-Liquid Crystal-Polymer Slices, POLICRYPS) overlaying a random distribution of plasmonic nanoparticles has been considered. Experiments evidence an anomalous discrete diffraction behavior in which light jumps from a waveguide to the adjacent one, thus moving into the two outermost lobes. Results support the hypothesis that the anomalous character of discrete diffraction is

mediated by plasmonic effects occuring at the interface between the AuNPs layer and the responsive waveguides. Indeed, light propagating in the guides (TM mode) excites a strong plasmonic dipolar field in the nanoparticles that prevents the liquid crystals thermal fluctuations hence preserving the periodical dielectric constant profile of the system during the propagation. The experimental analysis has been performed by changing the polarization and beam divergence of the impinging light, and the temperature of the sample. It turns out that the light propagation is strongly influenced by both polarization direction, intensity of the optical field of the propagating waves, and temperature variations. In the latter case, the stabilizing role of the plasmonic field on the liquid crystals orientation is particularly evident because the anomalous discrete diffraction pattern partly remains even in case the liquid crystals are expected in isotropic phase (e.g. at temperature above the nematic-isotropic transition point). Starting from the experimental evidence, we implemented a theoretical model able to interpret the active role of the liquid crystals, contained in the POLICRYPS, in their interaction with light contained in the POLICRYPS. This knowledge allows us to control light propagation characteristics in the waveguide (propagation length, kind of diffraction, ...) by acting on polarization, temperature, light intensity and divergence of the impinging light beam. The exchange of power between adjacent waveguides can be exploited in a number of thin-film photonic devices where it is required to control power division, modulation, switching and multi-plexing of optical signals.

Conflicts of interest

There are no conflicts to declare.

Acknowledgements

Authors are thankful to prof. Gaetano Assanto for the fruitful discussions.

This research was partially supported by the Air Force Office of Scientific Research (AFOSR), Air Force Research Laboratory (AFRL), U.S. Air Force, under grant FA9550-18-1-0038 (P. I. L. De Sio, EOARD 2017-2020) and the Materials and Manufacturing Directorate, AFRL.

Notes and references

1 H. Eisenberg, Y. Silberberg, R. Morandotti and J. Aitchison, *Physical Review Letters*, 2000, **85**, 1863.

2 R. Morandotti, H. Eisenberg, Y. Silberberg, M. Sorel and J. Aitchison, *Physical review letters*, 2001, **86**, 3296.

3 F. Lederer and Y. Silberberg, *Optics and Photonics News*, 2002, **13**, 48–53.

4 D. N. Christodoulides, F. Lederer and Y. Silberberg, *Nature*, 2003, **424**, 817–823.

5 A. Yariv, *IEEE Journal of Quantum Electronics*, 1973, **9**, 919–933.

6 D. Christodoulides and R. Joseph, *Optics letters*, 1988, **13**, 794–796.

7 M. J. Ablowitz, Z. H. Musslimani and G. Biondini, *Physical Review E*, 2002, **65**, 026602.

8 J. M. Bendickson, J. P. Dowling and M. Scalora, *Physical Review E*, 1996, **53**, 4107.

9 F. Lederer, S. Darmanyan and A. Kobyakov, *Spatial Solitons*, Springer, 2001, pp. 269–292.

10 A. L. Jones, *JOSA*, 1965, **55**, 261–271.

11 E. Fermi, J. Pasta and S. Ulam, *Los Alamos Report LA-1940*, 1955, **978**, year.

12 A. Yariv, *Optical electronics*, Saunders College Publ., 1991.

13 S. Suntsov, K. Makris, D. Christodoulides, G. Stegeman, A. Hache, R. Morandotti, H. Yang, G. Salamo and M. Sorel, *Physical review letters*, 2006, **96**, 063901.

14 G. I. Stegeman and M. Segev, *Science*, 1999, **286**, 1518–1523.

15 F. Lederer, G. I. Stegeman, D. N. Christodoulides, G. Assanto, M. Segev and Y. Silberberg, *Physics Reports*, 2008, **463**, 1–126.

16 G. Assanto, A. Fratalocchi and M. Peccianti, *Optics express*, 2007, **15**, 5248–5259.

17 A. Fratalocchi, G. Assanto, K. A. Brzdąkiewicz and M. A. Karpierz, *Optics express*, 2005, **13**, 1808–1815.

18 A. Fratalocchi, G. Assanto, K. A. Brzdąkiewicz and M. A. Karpierz, *Optics letters*, 2004, **29**, 1530–1532.

19 R. Caputo, A. De Luca, L. De Sio, L. Pezzi, G. Strangi, C. Umeton, A. Veltri, R. Asquini, A. d'Alessandro, D. Donisi, R. Beccherelli, A. Sukhov and N. Tabiryan, *Journal of Optics A: Pure and Applied Optics*, 2009, **11**, 024017.

20 R. Caputo, L. De Sio, A. Veltri, C. P. Umeton and A. V. Sukhov, *Journal of Display Technology*, 2006, **2**, 38.

21 M. Infusino, A. Ferraro, A. De Luca, R. Caputo and C. Umeton, *JOSA B*, 2012, **29**, 3170–3176.

22 A. Marino, F. Vita, V. Tkachenko, R. Caputo, C. Umeton, A. Veltri and G. Abbate, *The European Physical Journal E*, 2004, **15**, 47–52.

23 A. Veltri, L. Pezzi, A. De Luca and C. Umeton, *Optics express*, 2007, **15**, 1663–1671.

24 F. Simoni, *Nonlinear optical properties of liquid crystals and polymer dispersed liquid crystals*, World Scientific, 1997, vol. 2.

25 I.-C. Khoo, *Liquid crystals: physical properties and nonlinear optical phenomena*, John Wiley & Sons, 2007, vol. 64.

26 L. Pezzi, G. Palermo and C. Umeton, *Active Plasmonic Nanomaterials*, 2015, 1.

27 L. Pezzi, G. Palermo, A. Veltri, U. Cataldi, T. Bürgi, T. Ritacco, M. Giocondo, C. Umeton and A. De Luca, *Journal of Physics D: Applied Physics*, 2017, **50**, 435302.

28 G. Palermo, A. Guglielmelli, L. Pezzi, U. Cataldi, L. De Sio, R. Caputo, A. De Luca, T. Bürgi, N. Tabiryan and C. Umeton, *Liquid Crystals*, 2018, 1–7.

29 E. A. Marcatili, *Bell Labs Technical Journal*, 1969, **48**, 2071–2102.

30 H. Furuta, H. Noda and A. Ihaya, *Applied optics*, 1974, **13**, 322–326.

31 Y. Zhang, J.-z. Zhu and C.-p. Huang, *Physics Letters A*, 2016, **380**, 3949–3955.

32 L. Pezzi, A. De Luca, A. Veltri and C. Umeton, *Nonlinear Optics, Quantum Optics: Concepts in Modern Optics*, 2011, **43**, year.

33 M. Peccianti, A. De Rossi, G. Assanto, A. De Luca, C. Umeton and I. Khoo, *Applied Physics Letters*, 2000, **77**, 7–9.

34 A. Block, C. Etrich, T. Limboeck, F. Bleckmann, E. Soergel, C. Rockstuhl and S. Linden, *Nature communications*, 2014, **5**, year.

35 R. G. Hunsperger and J. R. Meyer-Arendt, *Applied Optics*, 1992, **31**, 298.

36 A. Boltasseva, T. Nikolajsen, K. Leosson, K. Kjaer, M. S. Larsen and S. I. Bozhevolnyi, *Journal of Lightwave technology*, 2005, **23**, 413.

37 L. De Sio, A. Veltri, A. Tedesco, R. Caputo, C. Umeton and A. V. Sukhov, *Applied optics*, 2008, **47**, 1363–1367.

38 A. Cunningham, S. Mühlig, C. Rockstuhl and T. Bürgi, *The Journal of Physical Chemistry C*, 2011, **115**, 8955–8960.

39 L. De Sio, U. Cataldi, A. Guglielmelli, T. Bürgi, N. Tabiryan and T. J. Bunning, *MRS Communications*, 2018, **8**, 550–555.

40 H.-S. Chu, W.-B. Ewe, E.-P. Li and R. Vahldieck, *Opt. Express*, 2007, **15**, 4216–4223.

41 N. Tabiryan, A. Sukhov and B. Y. Zel'Dovich, *Molecular Crystals and Liquid Crystals*, 1986, **136**, 1–139.

42 S. A. Maier and H. A. Atwater, *Journal of applied physics*, 2005, **98**, 10.

43 S. A. Maier, M. D. Friedman, P. E. Barclay and O. Painter, *Applied Physics Letters*, 2005, **86**, 071103.

44 M. Peccianti, C. Conti, G. Assanto, A. De Luca and C. Umeton, *Nature*, 2004, **432**, 733.

45 S. Trillo and W. Torruellas, *Spatial Solitons*, Berlin: Springer, 2001.

46 G. Assanto, M. Peccianti and C. Conti, *Optics and photonics news*, 2003, **14**, 44–48.

47 M. Peccianti, A. Dyadyusha, M. Kaczmarek and G. Assanto, *Nature Physics*, 2006, **2**, 737.

48 L. Pezzi, A. Veltri, A. De Luca and C. Umeton, *Journal of Nonlinear Optical Physics & Materials*, 2007, **16**, 199–206.

49 A. Yariv, *Optical electronics in modern communications*, Oxford University Press, USA, 1997, vol. 1.

50 P. Yeh, A. Yariv and C.-S. Hong, *JOSA*, 1977, **67**, 423–438.

51 D. Mandelik, H. Eisenberg, Y. Silberberg, R. Morandotti and J. Aitchison, *Physical review letters*, 2003, **90**, 053902.

52 P. S. J. Russell, *Applied Physics B: Lasers and Optics*, 1986, **39**, 231–246.

53 N. W. Ashcroft and N. D. Mermin, *Solid State Physics (Holt, Rinehart and Winston, New York, 1976)*, Holt, Rinehart Winston, New York, 1976.

54 H. Eisenberg, Y. Silberberg, R. Morandotti, A. Boyd and J. Aitchison, *Physical Review Letters*, 1998, **81**, 3383.

55 A. Yariv, *Optical Electronics*, Oxford University Press, 1990.

56 M. Conforti, M. Guasoni and C. De Angelis, *Optics letters*, 2008, **33**, 2662–2664.

57 G. L. Pedrola, *Beam Propagation Method for Design of Optical Waveguide Devices*, John Wiley & Sons, 2015.

58 J. Li, S. Gauza and S.-T. Wu, *Journal of applied physics*, 2004, **96**, 19–24.

59 J. Li and S.-T. Wu, *Journal of applied physics*, 2004, **96**, 170–174.

60 J. Li, C.-H. Wen, S. Gauza, R. Lu and S.-T. Wu, *Journal of Display Technology*, 2005, **1**, 51.

61 J. Li and S.-T. Wu, *Journal of applied physics*, 2004, **95**, 896–901.

62 L. Pezzi, G. Palermo, C. Umeton and A. De Luca, *Molecular Crystals and Liquid Crystals*, 2017, **649**, 31–37.

63 L. Pezzi, L. De Sio, G. Palermo, A. Veltri, T. Placido, M. L. Curri, N. Tabiryan and C. Umeton, Emerging Liquid Crystal Technologies XI, 2016, p. 97690C.

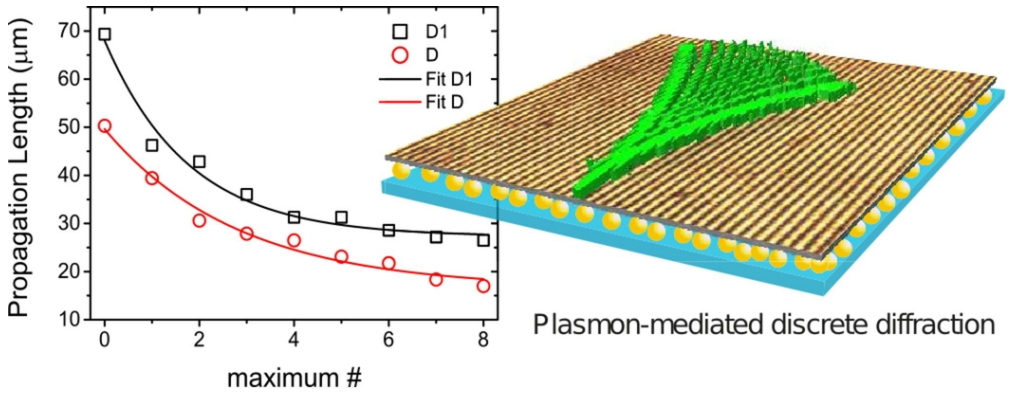

89x34mm (300 x 300 DPI)